

A Comparative Study of Reinforced Soil Shear Strength Prediction by the Analytical Approach and Artificial Neural Networks

Leila Arabet

Laboratory LMGHU
University of Skikda
Skikda, Algeria
arabet.leila@univ-jijel.dz

Mustapha Hidjeb

Civil Engineering Department
University of Skikda
Skikda, Algeria
mustapha_hidjeb@yahoo.fr

Faris Belaabed

Civil and Hydraulic Engineering Department
University of Jijel
Jijel, Algeria
bellabed.faris@univ-jijel.dz

Received: 4 October 2022 | Revised: 22 October 2022 and 25 October 2022 | Accepted: 27 October 2022

Abstract-For the prediction of the shear strength of reinforced soil many approaches are utilized which are complex and they depend on laboratory tests and several parameters. In this study, we aim to investigate and compare the ability of the Gray and Ohashi (GO) model and Artificial Neural Networks (ANNs) to predict the shear strength of reinforced soil. To achieve this objective, this work was divided into two parts. In the first part and in order to evaluate the impact of different fiber reinforcing parameters on the behavior of the soil, many direct shear experiments were carried out. The results revealed a significant improvement in shear strength values with fiber reinforcement. The increase in shear strength is a function of the fiber length, proportion, and direction. In the second part, we used the results of our experimental study to develop the ANN model. The obtained results agree reasonably well with the experiment ones, with very acceptable error (RMSE =1.714, MAE=5.981, $R^2=0.960$, and $E = -1.601\%$). The comparative study showed that the ANN model was more accurate and statistically more stable than the GO model, and the ANN model took all the conditions of the reinforced soil into one equation. On the other hand, the GO model does not take reinforcement failure and uses several equations.

Keywords-shear strength; reinforced soil; natural fibers; Gray & Ohashi model; artificial neural networks

I. INTRODUCTION

Soil instability can be dangerous and destructive. Soil reinforcement takes into consideration several factors, such as the reinforcement's form, texture, and rigidity [1], its cost-effectiveness, and its environmental friendliness [2-3]. In this work, we used soil reinforced by natural fibers. The prediction of its shear strength is necessary in order to study the soil behavior [1]. Different methods for estimating shear strength in

soils have occurred, generally based on variable theories such as force equilibrium [1, 4-5], statistical analysis [6-7], the approach of superposition of the effects of soil and fibers [8-9], and the energy dissipation approach [10-13]. Gray and Ohashi (GO) [1] suggested that with the addition of discrete fibers, physical and mechanical properties increase, and post-peak strength loss decreases. Based on the force equilibrium approach, the GO model established the shear strength of fiber-reinforced soil (τ_{ff}) as a combination of shear strength increment (ΔS) and unreinforced soil shear strength (τ_{ur}) parameters. The behavior of composite soils is complex since it depends on laboratory tests and many parameters [14]. In this regard, artificial intelligence methods such as the ANNs are promising and can be applied for the development of an approximate function that determines the shear strength under various conditions, considering the complexity of the approach models and the high cost of empirical experiments. During the recent years, the increased use of ANNs to tackle different engineering challenges has become popular in the domains of electronics [15-16], geophysics [17], hydraulics [18], etc. ANNs are used less in geotechnical engineering than in other domains even though there is success in solving such problems (e.g. prediction of pile deflection [19], bearing capacity of foundations [20], seismic deformation of rooted slopes [21], etc.).

The purpose of the current article is to investigate and compare the ability of the GO model and ANNs to predict the shear strength of soil reinforced with natural fibers. The results of the experimental program were utilized to develop the database used in the creation of the ANN structure. This research was carried out at the Laboratory of Civil and Environmental Engineering (LGCE) of the University of Jijel.

Corresponding author: Leila Arabet

www.etasr.com

Arabet et al.: A Comparative Study of Reinforced Soil Shear Strength Prediction by the Analytical ...

II. EXPERIMENTAL STUDY

A. Materials

Figure 1 presents the particle size analysis (according to NF P 94-056 and NF P 94-057). Table I describes the physical properties of the studied soil. The soil class is "Sm" according to the LPC code. Alfa fiber "esparto grass" was used as reinforcement. Table II describes its mechanical properties.

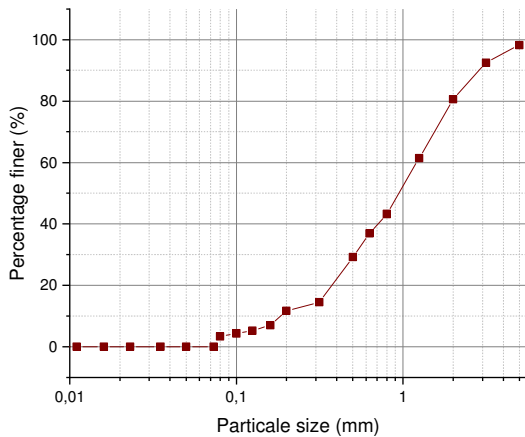


Fig. 1. Grain size distribution of the studied soil.

TABLE I. SOIL GEOTECHNICAL CHARACTERISTICS

Property	Value	Code
Sand equivalent E_s (%)	34	NF P 18-598
Water content (%)	25.85	NF P 94-050
Liquid limit (%)	8.27	NF P 94-051
Plastic limit (%)	1.00	NF P 94-051
Plasticity index (%)	7.27	NF P 94-051
Initial void ratio	0.521	
Methylene blue index (%)	0.215	NF P 94-068
Wet density (KN/m ³)	19	NF P 94-054
Specific gravity G_s	2.65	NF P 94-049

TABLE II. MECHANICAL PROPERTIES OF FIBERS USED [22]

Property	σ (GPa)	ϵ (%)	E (GPa)
Average value	63.83	3.12	2.05
Standard deviation	16.80	0.63	0.77
Coefficient of variance	26.31	20.12	37.55

TABLE III. OBTAINED RESULTS IN DIFFERENT ORIENTATIONS OF THE FIBERS

Direction	Fiber (%)	τ_{ff} (KPa) experimental			τ_{ff} (KPa) GO model [1]			Observation
		$\sigma_n = 100\text{KPa}$	$\sigma_n = 200\text{KPa}$	$\sigma_n = 300\text{KPa}$	$\sigma_n = 100\text{KPa}$	$\sigma_n = 200\text{KPa}$	$\sigma_n = 300\text{KPa}$	
Unreinforced	0.00	52.22	124	160.77	-	-	-	-
	0.25	65.85	170.97	177.91	70.78	121.17	182.04	
	0.50	60.20	111.07	191.41	73.24	137.86	198.54	
	0.75	89.27	187.37	267.82	80.67	141.60	205.69	
Vertical	1.00	79.94	142.75	205.70	101.18	170.60	238.12	$E = 2.89 \%$
	0.25	79.30	136.00	192.65	62.14	117.63	172.87	
	0.50	73.04	123.32	170.68	68.56	126.37	183.36	
	0.75	69.50	111.32	170.22	75.42	131.78	190.15	
Inclined	1.00	65.56	111.56	164.5	78.81	141.25	195.58	$E = 5.22 \%$
	0.25	78.32	152.5	214.04	59.57	114.25	169.74	
	0.50	71.49	134.61	246.57	61.36	116.62	171.76	
	0.75	71.43	170.10	211.28	63.06	120.55	174.79	
Horizontal	1.00	76.25	134.72	215.47	64.72	123.19	183.76	$E = -18.68 \%$

B. Experimental Procedure

Direct shear tests were conducted to a stainless metal box of a squared section of 6x6 cm² and 3cm high (according to NF P 94-071-1). The samples were prepared in undrained conditions and under normal stresses of 100, 200, and 300KPa (with 0.02mm/s loading velocity). Firstly, each sample was mixed with a constant fiber length of 1cm. After that, we added different fiber ratios ρ_f from 0 to 1% by weight of dry soil with a step of 0.25%, in different directions (horizontal, vertical, and inclined at 45°). Then, each sample was mixed with a constant fiber ratio. Then, we added different fiber lengths L_f from 1 to 2.5cm, with an increment step of 0.5cm in different directions (Figure 2).

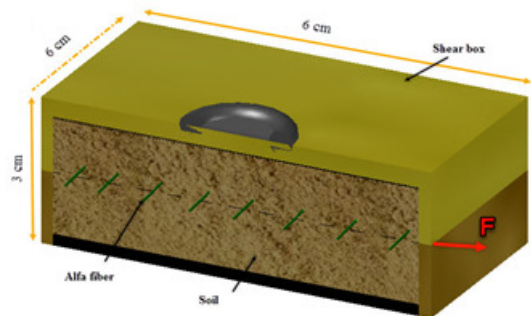


Fig. 2. Specimen preparation in the inclined direction of the alfa fibers.

C. Experimental Results

1) Variation in Fiber Ratio

From Table III, we can see that there is an improvement in shear strength relatively to the increase in reinforcements up to an optimum value. Above that, τ_{ff} decreases. These findings are consistent with those of [1, 14]. The average relative error (1) between the experimental results and the predicted results of shear strength from the GO model varies from 2.32 to -18.68%. The results show acceptable agreement between these two values.

$$E (\%) = \frac{1}{n} \sum_{i=1}^n \frac{\tau_{ff}(\text{experimental}) - \tau_{ff}(\text{predict})}{\tau_{ff}(\text{experimental})} (\%) \quad (1)$$

2) Variation of Fiber Length

The unreinforced soil's shear strength improves in each direction and is limited by the optimum fiber length (Table IV). The fiber direction changes the peak fiber length. This can be caused by the variation in the tensile fiber stress for each direction. The average relative error between the experimental results and the predicted results from the GO

model of shear strength varies from 18.16 to -7.56%. The results show acceptable agreement between these two values. In the vertical direction and at a length of 2.5cm, we observed a higher value of the error (= 59.69%). In this case, and during the test, we observed failure in the fibers. This inaccuracy can be explained by the fact that the GO model does not account for the plasticity of fibers.

TABLE IV. OBTAINED RESULTS IN DIFFERENT FIBER ORIENTATIONS OF DIFFERENT LENGTHS

Direction	Fiber (cm)	τ_{ff} (KPa) experimental			τ_{ff} (KPa) Gray & Ohashi			Observation
		$\sigma_n = 100\text{KPa}$	$\sigma_n = 200\text{KPa}$	$\sigma_n = 300\text{KPa}$	$\sigma_n = 100\text{KPa}$	$\sigma_n = 200\text{KPa}$	$\sigma_n = 300\text{KPa}$	
Unreinforced	0.00	52.22	124	160.77	-	-	-	-
Vertical	1.00	65.85	170.97	177.91	70.78	121.17	182.05	$E = 18.16\%$
	1.50	63.50	128.30	174.90	76.46	139.04	199.44	
	2.00	67.38	134.37	180.54	79.10	151.97	216.92	
	2.50	59.92	109.91	166.51	95.68	164.96	223.16	
Inclined	1.00	79.30	123.32	170.68	62.14	117.37	172.49	$E = -15.43\%$
	1.50	74.25	145.80	196.04	65.23	123.18	179.23	
	2.00	85.10	160.30	211.60	69.79	126.11	182.03	
	2.50	89.45	148.48	293.25	70.52	128.92	187.92	
Horizontal	1.00	78.32	152.50	214.04	59.57	114.25	169.74	$E = -7.56\%$
	1.50	68.87	161.30	207.22	60.49	115.25	171.13	
	2.00	58.32	115.30	161.37	61.56	117.01	171.58	
	2.50	54.25	129.05	162.60	68.00	117.39	174.68	

III. ARTIFICIAL NEURAL NETWORKS

Many studies have been conducted on the influence of ANN parameters, especially the activation function, on the ANN performance to assure good model generalization [23-24]. That is why in the current study, we used the growing technique [25]. The growing approach starts with a simple construction and then adds neurons and hidden layers until the performance is satisfactory. As a result, a huge number of simulations were run to determine the best ANN model design. For this, various ANN structures were trained with a different set of activation functions, numbers of hidden layers, and hidden neurons. For the learning algorithm, we used Levenberg-Marquardt (LM) back-propagation, which is the most commonly used for supervised learning [26].

A. Architecture of the Neural Network

The dataset that is utilized to create the neural network model is the product of the previous experiments. Of the 75 data samples, 70% are used for the training, and the algorithm to compute the validation error used the rest of the data. In this research, the model's inputs are the unreinforced soil's shear strength (τ_{ur}), the mobilized tensile strength of fibers (σ_f), the fiber ratio (ρ_f), the fiber length (L_f), and the angle of shear distortion (θ). According to experimental and theoretical studies, these input parameters are the most influential on the shear strength of reinforced soil [1], which is the output of our model (see Figure 3). As we mentioned above, we trained various architectures with different activation functions to obtain an optimum ANN model. In this study, sigmoid, tangent hyperbolic, and linear activation functions through one, two, three, and four-hidden layers with a different number of neurons were investigated.

The growing technique is the method employed in this study to determine the ideal architecture for a neural network model. As a result, we assume a certain number of hidden

layers and neurons at every layer. Then, we calculate the performance criteria (RMSE, MAE, and R^2) given by (2)-(4). If these are very satisfactory, it means that the chosen architecture is performing well. Otherwise, we change the number of hidden layers and neurons until performance criteria are satisfactory.

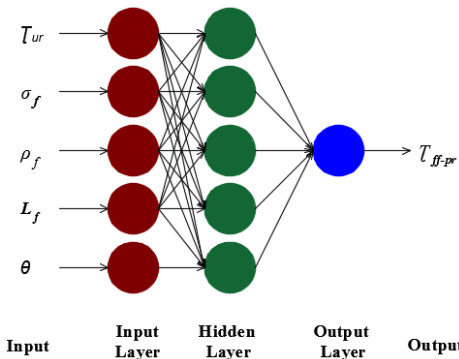


Fig. 3. The basic structure of the proposed ANN model.

$$R^2 = 1 - \left[\frac{\sum_1^n (\tau_{ff,pr} - \tau_{ff}(\text{experimental}))^2}{\sum_1^n (\tau_{ff}(\text{experimental}) - \text{ moy}(\tau_{ff}(\text{experimental})))^2} \right] \quad (2)$$

$$\text{MAE} = \frac{1}{n} \sum_{i=1}^n |\tau_{ff,pr} - \tau_{ff}(\text{experimental})| \quad (3)$$

$$\text{RMSE} = \sqrt{\frac{1}{n} \sum_1^n (\tau_{ff,pr} - \tau_{ff}(\text{experimental}))^2} \quad (4)$$

where $\tau_{ff,pr}$ and $\tau_{ff}(\text{experimental})$ are the predicted and the target values of shear strength of reinforced soil respectively.

B. Application of the Neural Network

Many simulations were carried out to find the best ANN model. We started with a simple structure and neurons and

hidden layers were added with various activation functions until the performance was adequate. Table V presents the architecture of the created MLPs. The best obtained models for each combination using different numbers of neurons are indicated.

C. Results and Discussion

Table VI shows the RMSE, MAE, and R² considering the training dataset, testing dataset, and all datasets in each best

ANN model. The last model (A15), which consists of 57 neurons and 4 hidden layers, performs best (see Figure 4). For A1, A2, and A11 models, the training was good but not enough to ensure good generalization ability. By considering the RMSE, MAE, and R² of models A7, A8, and A9, it can be concluded that the sigmoid transfer function in the output layer performs worse than other transfer functions.

TABLE V. DIFFERENT ARCHITECTURES OF MLP MODELS

ANN modes	Number of hidden layers	Number of neurons in hidden layers	Activation Function		Best ANN model
			Input	Output	
A1	1	1 to 30	Sigmoid	Linear	24
A2	1	1 to 30	Tangent Hyperbolic	Linear	12
A3	1	1 to 30	Linear	Linear	29
A4	1	1 to 30	Tangent Hyperbolic	Tangent Hyperbolic	2
A5	1	1 to 30	Linear	Tangent Hyperbolic	29
A6	1	1 to 30	Sigmoid	Tangent Hyperbolic	30
A7	1	1 to 30	Sigmoid	Sigmoid	25
A8	1	1 to 30	Tangent Hyperbolic	Sigmoid	25
A9	1	1 to 30	Linear	Sigmoid	6
A10	2	1 to 30 1 to 30	Tangent Hyperbolic Tangent Hyperbolic	Tangent Hyperbolic	3 - 19
A11	2	1 to 30 1 to 30	Tangent Hyperbolic Tangent Hyperbolic	Linear	4 - 9
A12	2	1 to 30 1 to 30	Linear Linear	Linear	8 - 11
A13	2	1 to 30 1 to 30	Linear Linear	Tangent Hyperbolic	8- 1
A14	3	1 to 30 1 to 30 1 to 30	Linear Linear Linear	Linear	3 - 9 - 6
A15	4	1 to 30 1 to 30 1 to 30 1 to 30	Tangent Hyperbolic Linear Linear Linear	Linear	12 - 10 - 25 - 10

TABLE VI. PREDICTION PERFORMANCE OF DIFFERENT ANN MODELS

	RMSE Training	MAE Training	RMSE Testing	MAE Testing	RMSE	MAE	E %	R ² Training	R ² Testing	R ²
A1	0.081	3.080	72.053	21.741	5.382	10.596	-3.664	0.992	0.820	0.886
A2	6.286	11.303	18.713	19.196	0.602	13.715	-0.253	0.938	0.827	0.900
A3	0.013	15.561	3.220	19.006	0.242	16.949	2.235	0.851	0.797	0.832
A4	0.002	33.104	4.506	38.780	0.293	34.839	11.550	0.339	0.262	0.318
A5	9.707	17.560	23.161	20.371	0.555	18.419	4.079	0.827	0.821	0.819
A6	63.194	16.608	24.453	28.551	4.613	20.257	0.287	0.903	0.492	0.757
A7	259.847	51.872	202.907	56.492	38.738	53.284	54.801	0.141	0.115	0.108
A8	321.020	46.351	231.911	53.502	46.635	48.536	58.461	0.554	0.344	0.501
A9	352.123	52.086	125.542	45.105	42.760	50.258	56.758	0.407	0.139	0.297
A10	38.635	25.309	59.366	21.533	7.662	24.155	-3.500	0.634	0.833	0.684
A11	8.993	10.752	23.499	23.085	0.648	14.520	1.090	0.938	0.748	0.879
A12	0.039	13.916	70.602	23.188	4.595	16.749	-0.645	0.894	0.802	0.833
A13	18.476	17.295	17.734	21.041	2.970	18.439	6.193	0.851	0.731	0.817
A14	15.639	18.039	18.039	21.197	16.069	0.155	17.437	0.806	0.892	0.836
A15	6.004	2.080	35.422	14.848	1.714	5.981	-1.601	0.998	0.891	0.960

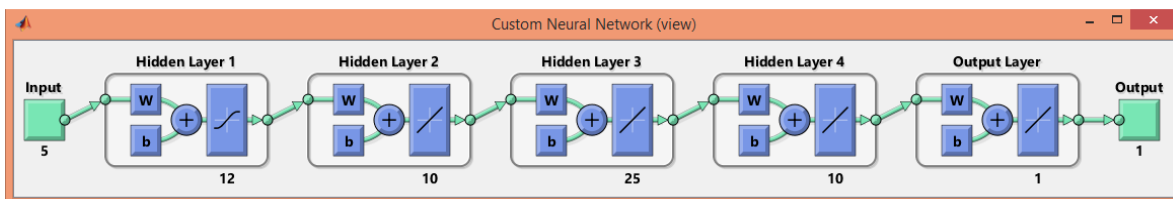


Fig. 4. The architecture of the optimal ANN model (A15).

Equations (5)-(9) are used to predict the shear strength of the reinforced soil:

$$\tau_{ff_pr} = \text{purelin.}(LW_{i4} \cdot A_i^4 + b_i^5) \quad (5)$$

$$[A_i^4] = \text{purelin.}(LW_{i3} \cdot A_i^3 + b_i^4) \quad (6)$$

$$[A_i^3] = \text{purelin.}(LW_{i2} \cdot A_i^2 + b_i^3) \quad (7)$$

$$[A_i^2] = \text{purelin.}(LW_{i1} \cdot A_i^1 + b_i^2) \quad (8)$$

$$[A_i^1] = \text{tansig.}(IW_i \cdot p + b_i^1) \quad (9)$$

where p is the matrix of inputs, $IW_i \cdot p$ is the weight matrix, representing the connection of the weights between the input layer neurons and the first hidden layer neurons, LW_{i1} is the weight matrix representing the connection of the weights between the first and the second hidden layer neurons, LW_{i2} is the weight matrix representing the connection of the weights between the second and the third hidden layer neuron, LW_{i3} is the weight matrix representing the connection of the weights between the third and the fourth hidden layer neurons, LW_{i4} is the weight matrix representing the connection of the weights between the fourth hidden layer neurons and the output neurons, $b_i^1, b_i^2, b_i^3, b_i^4$ and b_i^5 are the bias vectors of the first, second, third, and fourth hidden layer neurons, and the bias vector of the output layer respectively, $\text{purelin}(x) = x$, and $\text{tansig}(n) = \frac{2}{1+e^{-2n}} - 1$.

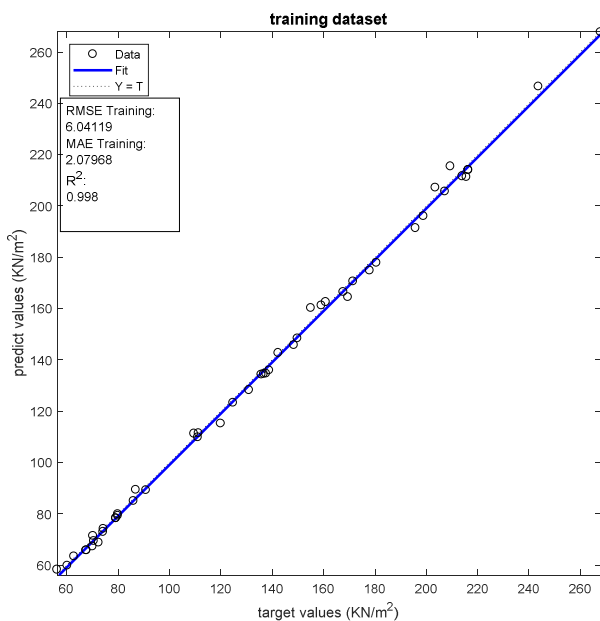


Fig. 5. Correlation results analysis of the model using the training data set.

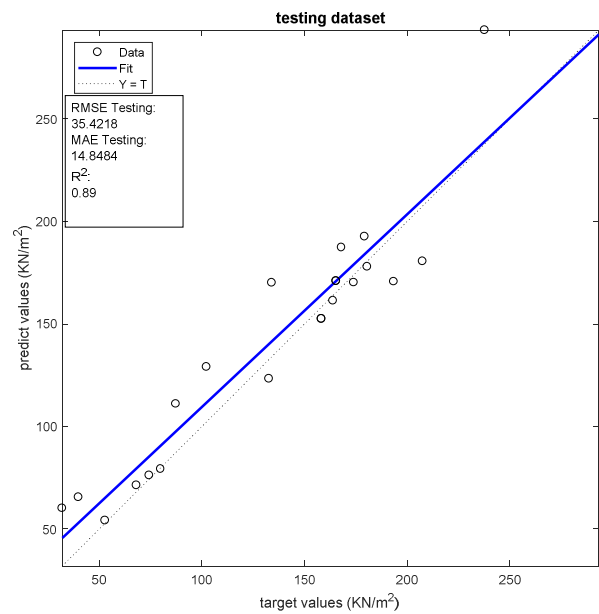


Fig. 6. Correlation results analysis of the model using the testing data set.

Figures 5 and 6 illustrate the training and testing data correlation between the target and predicted shear strength of reinforced soil using the optimal ANN model (A15). The values of RMSE (6.004), MAE (2.080), and R^2 (0.998) indicate that the target and predicted values for the training dataset are quite close. The testing dataset's RMSE (35.422), MAE (14.848), and R^2 (0.891) values are adequate proof that the proposed ANN model is the most reliable approach.

Because the shear strength of the reported instances in the dataset is different, we plotted the measured and estimated shear strength in Figure 7 against each other for all given cases. As shown in this Figure, the overall agreement between the predicted values obtained by the approximated function developed in this study and the values of the experimental model is indeed good, which is confirmed by the low values of RMSE (1.714), MAE (5.981), R^2 (0.960), and the relative average error value ($E = -1.601\%$).

Table VII presents the comparison between the GO model and the developed ANN model of this study. The different performance values (RMSE, MAE, R^2 , and E) obtained by the two models show that the optimum ANN model estimates the shear strength of reinforced soil more precisely than the GO model.

TABLE VII. COMPARISON BETWEEN THE PERFORMANCE VALUES OBTAINED BY THE GO MODEL AND THE DEVELOPED ANN MODEL

	Gray and Ohashi model				ANN developed model			
	RMSE	MAE	R^2	E (%)	RMSE	MAE	R^2	E (%)
Vertical	31.93	26.00	0.680	10.53	1.714	5.981	0.960	-1.601
Inclined	28.44	20.50	0.732	-5.10				
Horizontal	30.81	24.91	0.719	-13.12				

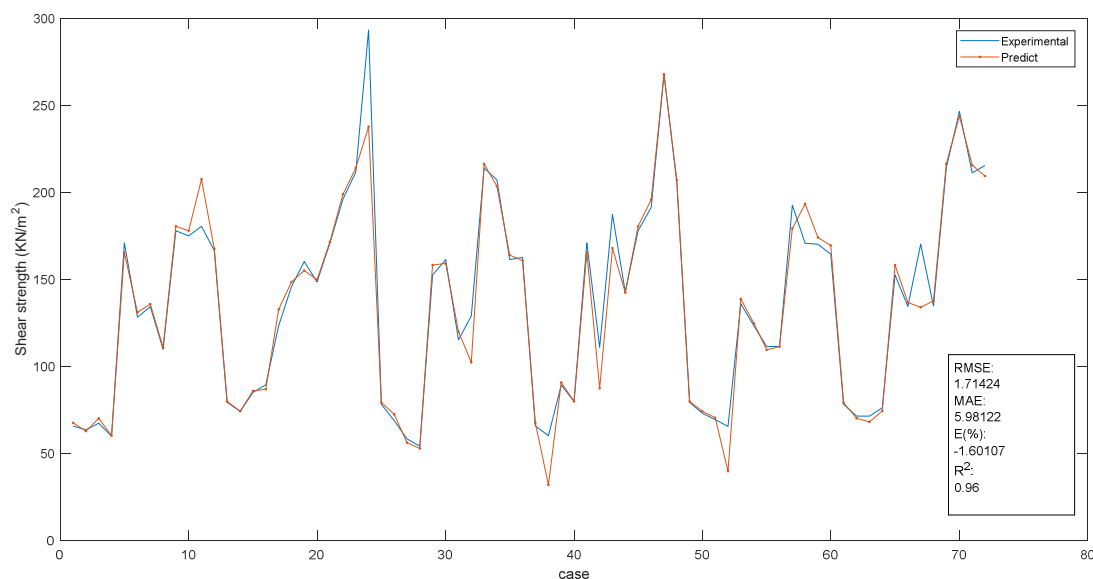


Fig. 7. Comparison of all experimental and predicted shear strengths evaluated by the ANN model of this study.

IV. CONCLUSION

An ANN model was built in this paper to predict the behavior of reinforced soil. The experimental results of the shear strength of reinforced soil was compared with the predicted results from the GO model and the ANN model. A parametric study to explain the impact of various factors on the behavior of reinforced soil was conducted. The main conclusions of this study are:

- The improvement of the shear strength of reinforced soil is not only influenced by the fiber length and ratio, but also by their direction.
- The fiber direction changes the optimal fiber ratio and the optimal fiber length. This can be due to the variation in fiber tensile stress for each direction.
- From the experimental study, the GO model does not take into account the plasticity of fibers.
- The shear strength of unreinforced soil (τ_{ur}), the mobilized tensile strength of fibers (σ_f), the fiber ratios (ρ_f), the fiber length (L_f), and the angle of shear distortion (θ) are the major factors influencing the behavior of reinforced soil, according to the parametric study and the theoretical analysis.
- The excellent agreement between the predictions of the optimal ANN model and the laboratory shear tests suggests that the developed model can quickly and conveniently predict the shear strength of reinforced soil for different values of reinforced parameters, which was confirmed by the values of RMSE (1.714), MAE (5.981), R^2 (0.960), and E (-1.601%).
- The developed optimal ANN model predicts the shear strength of reinforced soil more precisely than the GO model. Moreover, the GO model is based on many equations and it doesn't take into consideration the case of

the fiber failure. Instead, the proposed ANN model considers all conditions in one equation with minimal error and the best correlation. Therefore, the ANN model developed in this study is a robust and efficient alternative.

REFERENCES

- [1] D. H. Gray and H. Ohashi, "Mechanics of Fiber Reinforcement in Sand," *Journal of Geotechnical Engineering*, vol. 109, no. 3, pp. 335–353, Mar. 1983, [https://doi.org/10.1061/\(ASCE\)0733-9410\(1983\)109:3\(335\)](https://doi.org/10.1061/(ASCE)0733-9410(1983)109:3(335)).
- [2] R. Ramkrishnan, V. Karthik, M. R. Sruthy, and A. Sharma, "Soil Reinforcement and Slope Stabilization Using Natural Jute Fibres," in *Civil Infrastructures Confronting Severe Weathers and Climate Changes Conference*, HangZhou, China, Jul. 2018, pp. 130–143, https://doi.org/10.1007/978-3-319-95744-9_11.
- [3] S. M. Hejazi, M. Sheikhzadeh, S. M. Abtahi, and A. Zadhoush, "A simple review of soil reinforcement by using natural and synthetic fibers," *Construction and Building Materials*, vol. 30, pp. 100–116, May 2012, <https://doi.org/10.1016/j.conbuildmat.2011.11.045>.
- [4] R. A. Jewell and C. P. Wroth, "Direct shear tests on reinforced sand," *Geotechnique*, vol. 37, no. 1, pp. 53–68, Mar. 1987, <https://doi.org/10.1680/geot.1987.37.1.53>.
- [5] L. J. Waldron, "The Shear Resistance of Root-Permeated Homogeneous and Stratified Soil," *Soil Science Society of America Journal*, vol. 41, no. 5, pp. 843–849, 1977, <https://doi.org/10.2136/sssaj1977.03615995004100050005x>.
- [6] M. H. Maher and D. H. Gray, "Static Response of Sands Reinforced with Randomly Distributed Fibers," *Journal of Geotechnical Engineering*, vol. 116, no. 11, pp. 1661–1677, Nov. 1990, [https://doi.org/10.1061/\(ASCE\)0733-9410\(1990\)116:11\(1661\)](https://doi.org/10.1061/(ASCE)0733-9410(1990)116:11(1661)).
- [7] R. L. Michalowski and A. Zhao, "Continuum versus Structural Approach to Stability of Reinforced Soil," *Journal of Geotechnical Engineering*, vol. 121, no. 2, pp. 152–162, Feb. 1995, [https://doi.org/10.1061/\(ASCE\)0733-9410\(1995\)121:2\(152\)](https://doi.org/10.1061/(ASCE)0733-9410(1995)121:2(152)).
- [8] S. K. Shukla, N. Sivakugan, and A. K. Singh, "Analytical model for fiber-reinforced granular soils under high confining stresses," *Journal of Materials in Civil Engineering*, vol. 22, pp. 935–942, Sep. 2010, [https://doi.org/10.1061/\(ASCE\)MT.1943-5533.0000081](https://doi.org/10.1061/(ASCE)MT.1943-5533.0000081).
- [9] J. G. Zornberg, "Discrete framework for limit equilibrium analysis of fibre-reinforced soil," *Geotechnique*, vol. 52, no. 8, pp. 593–604, Oct. 2002, <https://doi.org/10.1680/geot.2002.52.8.593>.

- [10] R. L. Michalowski and A. Zhao, "Failure of Fiber-Reinforced Granular Soils," *Journal of Geotechnical Engineering*, vol. 122, no. 3, pp. 226–234, Mar. 1996, [https://doi.org/10.1061/\(ASCE\)0733-9410\(1996\)122:3\(226\)](https://doi.org/10.1061/(ASCE)0733-9410(1996)122:3(226)).
- [11] R. L. Michalowski and J. Cermak, "Triaxial Compression of Sand Reinforced with Fibers," *Journal of Geotechnical and Geoenvironmental Engineering*, vol. 129, no. 2, pp. 125–136, Feb. 2003, [https://doi.org/10.1061/\(ASCE\)1090-0241\(2003\)129:2\(125\)](https://doi.org/10.1061/(ASCE)1090-0241(2003)129:2(125)).
- [12] A. Diambra and E. Ibraim, "Fibre-reinforced sand: interaction at the fibre and grain scale," *Geotechnique*, vol. 65, no. 4, pp. 296–308, Apr. 2015, <https://doi.org/10.1680/geot.14.P.206>.
- [13] R. L. Michalowski, "Limit analysis with anisotropic fibre-reinforced soil," *Geotechnique*, vol. 58, no. 6, pp. 489–501, Aug. 2008, <https://doi.org/10.1680/geot.2008.58.6.489>.
- [14] S. K. Shukla, *Fundamentals of Fibre-Reinforced Soil Engineering*. New York, NY, USA: Springer, 2017.
- [15] L. T. H. Nhung, T. T. Phung, H. M. V. Nguyen, T. N. Le, T. A. Nguyen, and T. D. Vo, "Load Shedding in Microgrids with Dual Neural Networks and AHP Algorithm," *Engineering, Technology & Applied Science Research*, vol. 12, no. 1, pp. 8090–8095, Feb. 2022, <https://doi.org/10.48084/etasr.4652>.
- [16] N. T. T. Vu, N. P. Tran, and N. H. Nguyen, "Recurrent Neural Network-based Path Planning for an Excavator Arm under Varying Environment," *Engineering, Technology & Applied Science Research*, vol. 11, no. 3, pp. 7088–7093, Jun. 2021, <https://doi.org/10.48084/etasr.4125>.
- [17] A. Sokhal, Z. Benaissa, S. A. Ouadfeul, and A. Boudella, "Dynamic Rock Type Characterization Using Artificial Neural Networks in Hamra Quartzites Reservoir: A Multidisciplinary Approach," *Engineering, Technology & Applied Science Research*, vol. 9, no. 4, pp. 4397–4404, Aug. 2019, <https://doi.org/10.48084/etasr.2861>.
- [18] F. Belaabed, K. Goudjil, L. Arabet, and A. Ouamane, "Utilization of computational intelligence approaches to estimate the relative head of PK-Weir for submerged flow," *Neural Computing and Applications*, vol. 33, no. 19, pp. 13001–13013, Oct. 2021, <https://doi.org/10.1007/s00521-021-05996-7>.
- [19] K. Goudjil and L. Arabet, "Assessment of deflection of pile implanted on slope by artificial neural network," *Neural Computing and Applications*, vol. 33, no. 4, pp. 1091–1101, Feb. 2021, <https://doi.org/10.1007/s00521-020-04985-6>.
- [20] R. Nazir, E. Momeni, K. Marsono, and H. Maizir, "An Artificial Neural Network Approach for Prediction of Bearing Capacity of Spread Foundations in Sand," *Jurnal Teknologi*, vol. 72, no. 3, Jan. 2015, <https://doi.org/10.11113/jt.v72.4004>.
- [21] T. Liang, J. A. Knappett, A. Leung, A. Carnaghan, A. G. Bengough, and R. Zhao, "A critical evaluation of predictive models for rooted soil strength with application to predicting the seismic deformation of rooted slopes," *Landslides*, vol. 17, no. 1, pp. 93–109, Jan. 2020, <https://doi.org/10.1007/s10346-019-01259-8>.
- [22] M. Dallel, "Evaluation du potentiel textile des fibres d'Alfa (Stipa Tenacissima L.): caractérisation physico-chimique de la fibre au fil," Ph.D. dissertation, Haute-Alsace University, Mulhouse, France, 2012.
- [23] C. Ozkan and F. S. Erbek, "The Comparison of Activation Functions for Multispectral Landsat TM Image Classification," *Photogrammetric Engineering & Remote Sensing*, vol. 69, no. 11, pp. 1225–1234, Nov. 2003, <https://doi.org/10.14358/PERS.69.11.1225>.
- [24] I. S. Isa, Z. Saad, S. Omar, M. K. Osman, K. A. Ahmad, and H. A. M. Sakim, "Suitable MLP Network Activation Functions for Breast Cancer and Thyroid Disease Detection," in *Second International Conference on Computational Intelligence, Modelling and Simulation*, Bali, Indonesia, Sep. 2010, pp. 39–44, <https://doi.org/10.1109/CIMSiM.2010.93>.
- [25] M. T. Hagan, H. B. Demuth, and M. Beale, *Neural network design*. Boston, MA, USA: PWS Publishing, 1997.
- [26] J. J. Jeremiah, S. J. Abbey, C. A. Booth, and A. Kashyap, "Results of Application of Artificial Neural Networks in Predicting Geo-Mechanical Properties of Stabilised Clays—A Review," *Geotechnics*, vol. 1, no. 1, pp. 147–171, Sep. 2021, <https://doi.org/10.3390/geotechnics1010008>.